

Cite this: *Lab Chip*, 2012, 12, 3217–3220

www.rsc.org/loc

HIGHLIGHT

Research highlights

Šeila Selimović,^{ab} Sara Saedinia,^c Mehmet R. Dokmeci^{ab} and Ali Khademhosseini^{*abde}

DOI: 10.1039/c2lc90085h

Microfabricated microvasculature networks

Cells in their native environment obtain their nutrients and supplies through high density capillary networks. This is because transport through diffusion is insufficient to maintain cell survival for distances exceeding a few microns.¹ Hence the creation of thick tissue constructs necessitates the development of endothelialized vascular networks, which remains one of the major challenges in the field of tissue engineering.

To address this challenge, Cooper-White and colleagues have proposed a design based on a microfluidic vascular network.² This microfluidic device allows for rapid, uniform, and complete formation of an endothelial layer under continuous flow conditions by mimicking the equivalent *in vivo* tissue and its vasculature. A similar methodology had been applied previously by Weinberg *et al.*,³ however, in contrast to Weinberg's work, the work by Cooper-White ensured the generation of uniform physiological wall shear stresses throughout the microfluidic device, as well as a uniform velocity profile in all device channels.

The device structure was based on a multi-rung ladder network fabricated from poly(dimethylsiloxane) (PDMS) using conventional soft lithography techniques. It consisted of an input channel branching into a series of parallel micro-channels, which then culminated in a single output channel. A uniform velocity profile in all channels was achieved allowing uniform delivery of nutrients and oxygen to cells. In addition, the dimensions of the channels were designed to be similar to *in vivo* vascular channels in order to adequately mimic the structure of the vasculature. Finally, shear stress levels representative of the *in vivo* conditions were generated on the channel walls by carefully controlling the pressure differences inside the device. For example, a low and uniform shear stress on the order of 0.1 Pa could be generated in all channels simply by adjusting the on-chip flow to generate the desirable shear range for human umbilical vein endothelial cells (HUVECs). This approach generated a shear stress that was ten times smaller than in similar work³ and was suitable for continuous endothelialisation of the channels with HUVECs.

To visualize and assess the integrity of endothelialisation, immunofluorescence staining techniques were utilized. After coating the channel walls with fibrinectin, the vascular network was perfused for 24 h, and HUVECs were observed to attach, spread, and bridge corners inside the rectangular channels. This is particularly interesting since it had previously been suggested that the shear stress variation inside rectangular channels was detrimental to cell growth as opposed to rounded channels.⁴

Currently, this system is limited to short-term culture (72 h) due to the hydrophobic nature of PDMS. However,

the authors acknowledged that in the future they could either surface-treat PDMS or choose a more cell-friendly device material. Nevertheless, they succeeded in forming a 3D confluent network with a high degree of endothelialization compared to similar microfluidic vasculature platforms. The cells were observed to attach to the channel walls after 28 h of culture compared to several days in previous reports.⁵

The ability to rapidly assemble HUVECs to form microvasculature *in vitro* makes this an attractive platform for studies aimed at understanding the mechanisms of forming artificial vascular networks *in vitro* and eventually creating 3D tissues with vasculature. This is especially noteworthy, as the channel sizes on the device prototype were similar to the circulatory network *in vivo* and the device fabrication and operation is simple and well understood.

Decoupling mechanical and chemical cues in cell-based systems

Cells are known to alter their behavior in response to chemical and physical stimuli from their surroundings.⁶ To effectively engineer tissues *in vitro*, it is important to understand the biological basis of this response and to incorporate appropriate external cues into the cell culture platforms. Microscale techniques are particularly amenable to designing such studies, as they provide an excellent control of the external cues and allow for independent manipulation of different stimuli.⁷ However, the majority of lab-on-a-chip-based studies so far have been limited to testing topographical and chemical stimuli, since incorporating spatially and time-controlled mechanical

^aCenter for Biomedical Engineering, Department of Medicine, Brigham and Women's Hospital, Harvard Medical School, Cambridge, Massachusetts, 02139, USA

^bHarvard-MIT Division of Health Sciences and Technology, Massachusetts Institute of Technology, Cambridge, Massachusetts, 02139, USA

^cThe Henry Samueli School of Engineering, University of California, Irvine, California, 92697, USA

^dWyss Institute for Biologically Inspired Engineering, Harvard University, Boston, Massachusetts, 02115, USA.

E-mail: alik@rics.bwh.harvard.edu

^eWorld Premier International-Advanced Institute for Materials Research (WPI-AIMR), Tohoku University, Sendai, 980-8577, Japan

cues, *e.g.* via chips with moving parts, is far more technically challenging.

To address this issue, Antaki, LeDuc and colleagues have developed an innovative microscale solution that allows for independent control of mechanical and chemical stimuli to single cells. In their work, Ruder *et al.*⁸ created an open glass platform, onto which they loaded a single cell and pinned it underneath a movable fiber for mechanical actuation. More specifically, a polypropylene scaffold consisting of three fibers (pin, central and actuation fiber) was attached to a glass slide with PDMS as glue (Fig. 1a,b). A single cell was then placed onto the fibronectin-coated glass slide, such that it attached to the actuation fiber. When this fiber was displaced using a needle, the upper side of the cell was displaced as well, causing the cell to stretch (Fig. 1c). The amount of stretch could be controlled by changing the location of the cell underneath the actuation fiber. Namely, its displacement varied with the distance from the pin fiber (Fig. 1d–f). If required, a chemical solution could be added on top of the scaffold prior to or after the mechanical testing, thereby providing an alternative, independent observation of the cellular response.

The proof-of-concept study was conducted with NIH-3T3 fibroblasts. First, cells were cultured on the chip for 1–2 days and allowed to migrate and attach to the fiber scaffold. When observed under an optical microscope, cells which attached to the fibers were seen to have stellate morphologies, while unattached cells were planar and had a distinct nuclear bulge. Furthermore, the distribution of the actin cytoskeleton was wider along the *z*-axis in cells attached to the fiber, than in surface-confined cells, again indicating the 3D cell structure. Finally, the calcium signaling response of cells loaded with a synthetic calcium dye and exposed to mechanical and chemical stimuli was measured by analyzing the fluorescence intensity of the cells. A brief increase in calcium concentration was observed after a critical stretch magnitude was applied to the cells. The subsequent addition of ATP led to a longer-lasting calcium increase with dynamics revealing that calcium signaling pathways remained intact after the stretch.

A major benefit of this experimental approach is that it provides an opportunity for testing cells in 3D. Certain cells, such as fibroblasts, are known to exhibit

different morphologies in 2D and 3D environments, and although the cells in this case are confined to a flat surface, pinning them to an elevated fiber provides the 3rd dimension. Next, the chemical signal could be applied independent of the mechanical stretch, simply by exchanging the chemical solution bathing the pinned cell. This results in a more accurate measurement of the cell response than, for example, in 3D cell-encapsulating hydrogels, which can interfere with the chemical. Furthermore, this method is compatible with optical microscopy methods, and since only a single cell is tested at a time, there is no need for confocal imaging. Also, the fabrication of this platform is simple, fast and cheap. Parallelizing the system for simultaneous observation of multiple cells, as well as adding microfluidic perfusion structures, could result in a chip that serves the needs of a range of biological and bioengineering studies.

Chitosan nanoparticles for fuel cell membranes

Fuel cells convert chemical energy of hydrogen-oxygen reactions into electrical

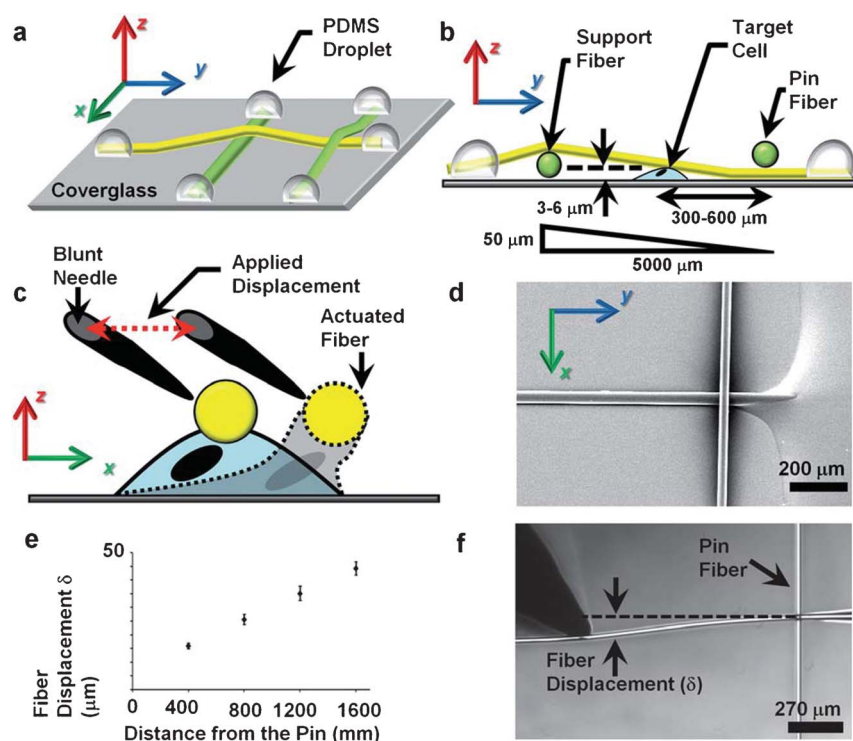


Fig. 1 a) and b) The minimal-profile 3-dimensional (MP3D) device for mechanical actuation and chemical testing of single cells; c) and d) the actuation mechanism; e) the actuation fiber displacement. Figure reprinted from Ruder *et al.*⁸ with permission from the Royal Society of Chemistry.

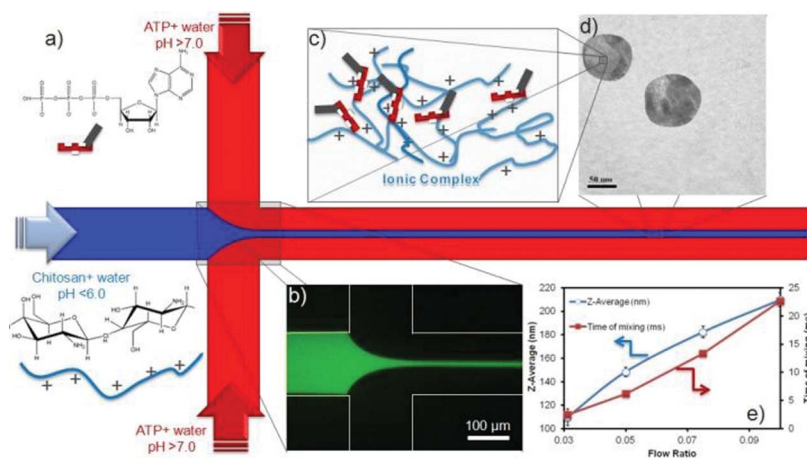


Fig. 2 The flow focusing setup (a,b) used for generating chitosan nanoparticles crosslinked with ATP (d) and the schematic representation of the gelled particles (c). Reprinted from Majedi *et al.*¹¹ with permission from the Royal Society of Chemistry.

energy, by means of electrolyte ions, which move between a cathode and an anode. Some fuel cells utilize proton exchange membranes, which conduct only protons, but not electrons.⁹ A material of choice for these membranes is the synthetic polymer Nafion, as it offers controllable proton conductivity. However, Nafion can be porous to fuel, as well. This characteristic can be modified by the inclusion of fillers in the Nafion membrane, as long as these fillers do not diminish the conductivity of protons.¹⁰

The approach taken by Renaud and coworkers is centered on the inclusion of chitosan nanoparticles into the Nafion membrane to limit the membrane pore size and increase the proton conductivity. Majedi *et al.*¹¹ used a standard flow focusing, PDMS-based setup to fabricate chitosan nanoparticles. The chitosan solution was delivered in the core flow, and the sheath flow consisted of an aqueous adenosine triphosphate (ATP) solution (Fig. 2a–b). The most common ionic crosslinker for chitosan gelation is sodium tripolyphosphate, however the researchers chose ATP for its adenine groups, which can improve the proton conductivity of the resulting fuel cell membrane.

Interestingly, the core and sheath flow rates were chosen in the jetting, rather than the drop-making region. The novelty of this approach is that ATP diffused into and mixed with the chitosan solution to nucleate particles on the order of 100 nm. This particle size can otherwise only be reached by using sub-micron sized nozzles

and very high flow rate ratios, which is less efficient. It was observed that the mixing time of the two solutions, controlled by the flow rate, affected the droplet and particle size. Namely, comparatively high flow rates ($\sim 1\text{--}10\ \mu\text{L min}^{-1}$) resulted in a mixing time on the order of a few ms and produced smaller particles, while flow rates that were one order of magnitude lower required a longer mixing time and created larger particles. The crosslinked chitosan nanoparticles ranged in size from ~ 100 to $200\ \text{nm}$, similar in dimensions to the ones fabricated by other fabrication techniques, *e.g.* flash mixing. The two flow rates also affected the amount of surface charges on the particles. An increase in the flow rates caused a reduction in surface charges and therefore in Zeta potential of the particles, since the manufactured particles had a small surface. Still, this method produced nanoparticles with at least 20% more surface charges than bulk mixing. Last, a constraint placed on this microfluidic nanoparticle fabrication method required that the chitosan-ATP mixing time be shorter than the gelation time. This would ensure that the particles were stable and more homogeneous in size than particles generated by bulk mixing.

The crosslinked chitosan-ATP nanoparticles were incorporated into a Nafion membrane using solvent casting, at a 2% weight fraction. The filled Nafion membrane had four times lower permeability to oxygen than an unfilled membrane, indicating that employing

chitosan-based nanoparticles as fillers could potentially also reduce the permeation of fuel. In addition, the conductivity of the filled membrane was higher than the unfilled membrane, and also increased with the temperature. Here, the largest gain was made with the smallest nanoparticles ($100\text{--}120\ \text{nm}$), most likely due to their comparatively large surface area and the high number of surface charges. This led to an improvement in fuel cell performance, expressed as a 3-fold increase in maximum power output compared to traditional Nafion-based fuel cell membranes. The filled membrane could be used continuously for over 100 h with high performance stability.

The present work is noteworthy for its creative application of a flow-focusing setup to generate nanoparticles with a narrow size distribution. A similar approach could be used for the fabrication of materials with novel physical properties. It also serves as an example for the diversity in the use of microfluidics, which include membrane development and energy applications.

References

- 1 J. Folkman and M. Hochberg, *J. Exp. Med.*, 1973, **138**, 745–753.
- 2 L. T. Chau, B. E. Rolfe and J. J. Cooper-White, *Biomicrofluidics*, 2011, **5**, 034115.
- 3 E. J. Weinberg, J. T. Borenstein, M. R. Kaazempur-Mofrad, B. Orrick and J. P. Vacanti, *MRS Online Proc. Libr.*, 2004, **820**, 6.
- 4 J. Borenstein, M. Tupper, P. Mack, E. Weinberg, A. Khalil, J. Hsiao and G. García-Cardena, *Biomed. Microdevices*, 2010, **12**, 71–79.

-
- 5 M. K.-M. C. Fidkowski, J. Borenstein, J.P. Vacantim, R. Langer and Y. Wang, *Tissue Eng.*, 2005, **11**, 302.
- 6 (a) P. A. Janmey and C. A. McCulloch, *Annu. Rev. Biomed. Eng.*, 2007, **9**, 1–34; (b) J. Y. Wong, J. B. Leach and X. Q. Brown, *Surf. Sci.*, 2004, **570**, 119–133.
- 7 S. A. Vanapalli, M. H. G. Duits and F. Mugele, *Biomicrofluidics*, 2009, **3**, 012006.
- 8 W. C. Ruder, E. D. Pratt, S. Bakhru, M. Sitti, S. Zappe, C.-M. Cheng, J. F. Antaki and P. R. LeDuc, *Lab Chip*, 2012, **12**, 1775–1779.
- 9 S. Gamburzev and A. J. Appleby, *J. Power Sources*, 2002, **107**, 5–12.
- 10 M. A. Hickner, H. Ghassemi, Y. S. Kim, B. R. Einsla and J. E. McGrath, *Chem. Rev.*, 2004, **104**, 4587–4612.
- 11 F. S. Majedi, M. M. Hasani-Sadrabadi, S. H. Emami, M. Taghipoor, E. Dashtimoghdam, A. Bertsch, H. Moaddel and P. Renaud, *Chem. Commun.*, 2012, **48**, 7744–7746.